
Warm brine lakes in craters of active mud volcanoes, Menes caldera off NW Egypt: evidence for deep-rooted thermogenic processes

Stéphanie Dupré^{1, *}, Jean Mascle², Jean-Paul Foucher¹, François Harnegnies¹, John Woodside³,
Catherine Pierre⁴

¹ IFREMER, Géosciences Marines, 29280, Plouzané Cedex, France

² Observatoire Océanologique, BP48, 06235, Villefranche-sur-mer, France

³ Vrije Universiteit, De Boelelaan 1085, 1081 HV, Amsterdam, The Netherlands

⁴ Université Pierre et Marie Curie, LOCEAN (UMR 7159), 4 Place Jussieu, 75252, Paris Cedex 05, France

*: Corresponding author : Stéphanie Dupré, email address : stephanie.dupre@ifremer.fr

Abstract:

The Menes caldera is a fault-controlled depression (~8 km in diameter) at ~3,000 m water depth in the western province of the Nile deep-sea fan off NW Egypt, comprising seven mud volcanoes (MVs) of which two are active. Based on multichannel and chirp seismic data, temperature profiles, and high-resolution bathymetric data collected during the 2000 Fanil, 2004 Mimes and 2007 Medeco2 expeditions, the present study investigates factors controlling MV morphology, the geometry of feeder channels, and the origin of emitted fluids. The active Cheops and Chephren MVs are 1,500 m wide with subcircular craters at their summits, about 250 m in diameter, generally a few tens of metres deep, and filled with methane-rich muddy brines with temperatures reaching 42 °C and 57 °C respectively. Deployments of CTDs and corers with attached temperature sensors tracked these warm temperatures down to almost 0.5 km depth below the brine lake surface at the Cheops MV, in a feeder channel probably only a few tens of metres wide. Thermogenic processes involve the dissolution of Messinian evaporites by warm fluids likely sourced even deeper, i.e. 1.7 and 2.6 km below the seabed at the Cheops and Chephren MVs respectively, and which ascend along listric faults. Seepage activity appears broadly persistent since the initiation of mud volcanism in the Early Pliocene, possibly accompanied by lateral migration of feeder channels.

1. Introduction

Seep-related structures including pockmarks and mud volcanoes (MVs) have been reported in various tectonic settings (see reviews in Kopf 2002; Dimitrov and Woodside 2003; Judd and Hovland 2007), from divergent (e.g. Neurauter and Roberts 1994; Sager et al. 2003; Loncke et al. 2004; Gay et al. 2007; van Rensbergen et al. 2007; Paull et al. 2008; Ho et al. 2012) to convergent plate margins (e.g. Cita et al. 1981; Langseth et al. 1988; Wiedicke et al. 2001; Capozzi and Picotti 2002; Zitter et al. 2006). Mud volcanism preferentially occurs in deltaic and accretionary prism settings where overpressured deep fluids (water and gas) migrate upwards due to buoyancy, carrying solid particles (cf. Kopf 2002; Deville et al. 2006). Expelled material most commonly involving water, gas, liquid hydrocarbons, mud and rock clasts can produce MVs both on the seafloor and on land. Deep seismic soundings indicate that mud volcanoes generally have a deep origin (at least a few kilometres in depth; e.g. Loncke et al. 2004; Davies and Stewart 2005; Deville et al. 2006). The origin of the emitted gases (e.g. thermogenic, biogenic) can be determined by isotopic analyses (Whiticar 1999; Deville et al. 2003; Bourry et al. 2009). Dating of rock clasts and sediments brought to the surface during eruption provides stratigraphic constraints on their deep sources (Camerlenghi et al. 1992; Praeg et al. 2009; Giresse et al. 2010).

In sedimentary basins characterized by evaporite deposits, seepage may be associated with highly concentrated brines. Seafloor brines have been reported in the Red Sea (Pautot et al. 1984; Hartmann et al. 1998), the Mediterranean Sea, here mainly along the Mediterranean Ridge (de Lange et al. 1990; Charlou et al. 2003; Huguen et al. 2005; Cita 2006; Aiello et al. 2012) with a few sites in the Nile deep-sea fan (Foucher et al. 2009; Huguen et al. 2009), and in the Gulf of Mexico (Shokes et al. 1977; MacDonald et al. 1990, 2000; Joye et al. 2005, 2009; Pilcher and Blumstein 2007; Bernard et al. 2007). They accumulate in seafloor depressions of various scales (m to km), such as anoxic collapsed basins (e.g. the Tyro, Bannock, Urania, Atalante and Discovery basins along the Mediterranean Ridge, and the Orca Basin in the Gulf of Mexico), pockmarks (e.g. metre-scale brine pools in the Olimpi mud volcano field in the eastern Mediterranean), and the craters of mud volcanoes (e.g. larger lakes at sites AC601, GB233 and GB245 on the Gulf of Mexico continental slope, and the Cheops and Chephren mud volcanoes on the Nile deep-sea fan). Brine seepage associated with methane venting occurs at several MVs discovered so far in the Gulf of Mexico (MacDonald et al. 1990, 2000; Joye et al. 2005, 2009) and the eastern Mediterranean (Charlou et al. 2003; Huguen et al. 2005, 2009; Cita 2006; Borin et al. 2009; Aiello et al. 2012; Prinzhofer and Deville 2013). Brine seepage there is obviously related to fluid venting of mud volcanoes (MacDonald et al. 1990; Cita 2006).

Muddy brines are hypersaline (2 to 8 times more concentrated than ambient seawater; MacDonald et al. 2000; Charlou et al. 2003; Huguen et al. 2009; Table 1), gas-rich solutions enriched by very fine particles (MacDonald et al. 2000; Huguen et al. 2009; Aiello et al. 2012; Pierre et al. 2014, this volume) and characterized by intense microbial activity at the seawater–brine interface and deeper within the brines (Omorigie et al. 2008; Joye et al. 2009). Brine pools and lakes at mud volcanoes are not only scarce but also extremely difficult to sample by means of, for example, submersibles and remotely operated vehicles (ROVs) which have proven very efficient in cold seep environments. Moreover, brine seepage is highly variable in both space and time in response to its dynamics. It is not surprising, therefore, that muddy brine seeps are overall poorly documented, except in the Gulf of Mexico and along the Mediterranean Ridge where the few geophysical studies dealt mainly with high-resolution sonar image acquisitions (Woodside and Volgin 1996; Huguen et al. 2005; Joye et al. 2005; Foucher et al. 2009). Indeed, knowledge of the geometry of brine lakes and their feeder channels is still largely rudimentary.

On the Nile deep-sea fan, brine seepage in association with mud volcanism has been investigated over the last decade within the framework of the MEDIFLUX and HERMES programmes during the Nautinil (Huguen et al. 2009), Mimes (Woodside et al. 2004) and Medeco2 (Pierre et al. 2008; Foucher et al. 2009) expeditions. The present study focuses on the geophysical characterization of muddy brine lakes in the craters of active gas-emitting MVs within the 8 km wide collapsed Menes caldera off NW Egypt in the western province of the Nile deep-sea fan (Fig. 1), based on hitherto unpublished chirp and seismic profiles as well as deep high-resolution temperature records. Incorporating the findings of earlier work for this study region (see below), the ultimate aim was to improve our understanding of the dynamics of mud volcanism by exploring mud volcano morphology, as well as the geometry of feeder channels and the origin of emitted fluids associated with brine lakes.

2. Geological setting

The Nile deep-sea fan, which has undergone rapid burial under high rates of subsidence and sedimentation since the Late Miocene, comprises a thick pile of clastic sediments from the river Nile (Aal et al. 2001; Dolson et al. 2001; Caméra et al. 2010). The fan hosts numerous active fluid-escape structures characterized by mud volcanism, gas escape into the water column, brine seepage, the development of benthic chemosynthetic ecosystems and authigenic carbonate precipitation (Loncke et al. 2004; Dupré et al. 2007, 2008b, 2010; Gontharet et al. 2007; Duperron et al. 2008; Omoregie et al. 2008; Bayon et al. 2009, 2013; Huguen et al. 2009; Feseker et al. 2010; Nuzzo et al. 2012; Prinzhofer and Deville 2013; Mascle et al. 2014; Pierre et al. 2014, this volume; Fig. 1). The deepest part (2,500–3,000 m water depth) of the fan's western province hosts a 50 by 100 km wide field of mud volcanoes comprising one of the most striking seep-related structures yet discovered in the region—the Menes mud volcano caldera complex, at the foot of the continental slope in water depths around ~3,000 m (Loncke et al. 2004; Huguen et al. 2009; Fig. 2). This 8 km wide caldera, the largest known collapse structure associated with brine seepage and mud volcanism (cf. Praeg et al. 2009 and Dupré et al. 2010 for the 2–3 km wide caldera structures known elsewhere in the eastern Mediterranean, and Bonini 2008 for the 500 m wide onshore Nirano caldera MV field in the Northern Apennines), lies ~100 m below the surrounding seafloor, i.e. at 3,020 m water depth.

The Menes caldera encompasses seven mud volcanoes—Chephren, Cheops, Mykerinos, Menitites, and three unnamed ones (Fig. 3). The former two are active. At the summits, the craters of the active Chephren and Cheops MVs have well-delimited brine lakes explored by near-bottom surveys with the Nautile submersible (Nautinil cruise in 2003; Huguen et al. 2009) and the Victor6000 ROV (remotely operated vehicle; Medeco2 cruise in 2007; Pierre et al. 2014, this volume; Fig. 4). Based also on high-resolution seabed mapping (Foucher et al. 2009; Mascle et al. 2014; Pierre et al. 2014, this volume), the brine lakes are subcircular with a diameter of 250 m, these being the largest of their kind documented to date (cf. MacDonald et al. 1990, 2000; Huguen et al. 2005; Bernard et al. 2007). Woodside and Volgin (1996) identified a 260 m wide brine lake along the Mediterranean Ridge but it did not appear related to mud volcanism.

The muddy brines of the Cheops and Chephren crater lakes are characterized by clay-size particles, a strong H₂S smell (0.2 and 0.5–7.2 mmol l⁻¹ respectively), as well as high methane levels (up to 2.3 and 5.6 mmol per litre of wet sediment respectively) and salinities (up to 310 and 153 PSU respectively), the latter well above the background value (38 PSU) for Mediterranean bottom seawater (Table 1; de Lange et al. 2006; Pierre et al. 2008, 2014 in this volume; Huguen et al. 2009) and below the saturation level (350 PSU for brines containing only Na⁺ and Cl⁻ ions). At both MVs, the overlying water column is saturated with methane (Woodside et al. 2004; Pierre et al. 2008; Prinzhofer and Deville 2013). At mud

volcanoes in the western Nile province, including the Cheops and Chephren MVs, methane-derived carbonates precipitate as carbonate crusts at the seafloor, and concretions within the subseafloor sediments and the brine lakes (Gontharet et al. 2007; Pierre et al. 2014, this volume). Moreover, the brine lake surface at both MVs is colonized by dense white bacterial filaments (Huguen et al. 2009, Fig. 4) identified as sulphide-oxidizing bacteria by Omoregie et al. (2008).

By contrast, the crater at the summit of the non-active Mykerinos MV is today devoid of brine. However, the crater bottom is characterized by authigenic carbonates and a thin pelagic cover containing dense shell debris (Gontharet et al. 2007; Huguen et al. 2009), pointing to past fluid-venting activity. Abundant euhedral gypsum crystals support the existence of a former brine lake at the Mykerinos MV, while low $\delta^{18}\text{O}$ values (down to 0.6‰) of carbonate concretions in subseafloor sediments at the bottom of the Mykerinos crater may indicate precipitation in warm fluids (Gontharet et al. 2007).

The Menes caldera is a fault-controlled depression (Loncke et al. 2004; Huguen et al. 2009) within the extensional domain of the Messinian salt gliding system, roughly at the foot of a growth fault system (Gauillier et al. 2000; Loncke et al. 2006). Although salt commonly acts as a seal preventing upward flow of fluids (e.g. in the western Mediterranean Sea), salt tectonics can dissect the sedimentary pile and create faults which form fluid migration pathways (Masclé et al. 2014, this volume). Most MVs in the western Nile province are located either in areas where the salt is nearly absent or above growth faults (see Fig. 6 in Loncke et al. 2004).

Brine seepage at the Menes caldera is, therefore, the seabed manifestation of deep-rooted processes inherently associated with high temperatures. Indeed, temperatures reaching 57 °C have been recorded down to 250 m below the seawater–brine interface in the Chephren MV brine lake, with corresponding evidence of 25–42 °C already at 10 m depth in the neighbouring Cheops MV brine lake (2004 Mimes expedition, Woodside et al. 2004; de Lange et al. 2006). Low $\delta^{18}\text{O}$ values (down to –2.8‰) of authigenic carbonates at the Cheops and Mykerinos MVs support their precipitation in warm fluids of deep origin (Gontharet et al. 2007; Pierre et al. 2014, this volume). Moreover, the geochemical/isotopic signatures of gases emitted by the two MVs indicate a predominance of methane (88.3 mol/mol% at Chephren MV) of mostly thermogenic origin with a possible microbial contribution (Prinzhofer and Deville 2013), also supported by $\delta^{13}\text{C}$ signatures from carbonates (Gontharet et al. 2007; Pierre et al. 2014, this volume). The underlying Messinian evaporites (Hsü et al. 1973) are the likely source of the high-salinity brines in the Chephren and Cheops MVs (Gontharet et al. 2007; Huguen et al. 2009; Pierre et al. 2014, this volume). The chemical signatures of brines in the anoxic basins of the Mediterranean Ridge indicate a similar dissolution of Messinian evaporites (Cita 2006). Based on high-quality 2D and 3D seismic data, Bentham et al. (2006) argued that mud volcanism is related to the withdrawal and mobilization of overpressured Tortonian shales which lie immediately beneath an important regional unconformity at the base of the Messinian evaporites. Giresse et al. (2010) reported rock clasts of Late Cretaceous age in short (<10 m long) cores collected ~30 km from the Menes caldera.

This wealth of ever-increasing information well reflects the Egyptian offshore region being now recognized as a prolific hydrocarbon domain (Dolson et al. 2002). The main reservoirs are found in Pliocene-Pleistocene deepwater channels and basin-floor turbidite sands, as well as in Late Miocene sequences composed of fluvial and turbidite sands, with Mesozoic and Oligocene source rocks (Aal et al. 2001; Dolson et al. 2001; Vandr e et al. 2007).

3. Materials and methods

High-resolution multichannel seismic data were acquired during the Fanil expedition of 2000 using two 75 cubic inch Soderia mini-GIs and five GI airguns with 24-channel streamers (for more information, see Bellaiche et al. 2001; Loncke 2002). Two N30–40 oriented seismic profiles crossing the Menes caldera and imaging the structures to a subseafloor depth of 2 s two way travel time (TWT) are reported in this paper. These profiles, 23 and 26 km long, were processed by Alain Moreau (Géosciences Azur, Villefranche-sur-mer, France).

Chirp profiles were acquired during the 2004 Mimes (3.5 kHz Oretch 3010) and 2007 Medeco2 (1.8–5.3 kHz Echoes Ixsea) expeditions from onboard the R/V *Pelagia* and R/V *Pourquoi pas?* respectively. Several lines were run across the Cheops, Chephren, Menitites and Mykerinos MVs, a selection of which are reported here. The Mimes profiles were recorded only on paper and were not processed further because no digital records were available. The Medeco2 chirp profile was processed using Subop, a Matlab-based software developed by Anne Pacault (Ifremer, Plouzané, France). Based on regional knowledge (e.g. the Napoli MV area, Robertson et al. 1996) and background values for Mediterranean pelagic and hemipelagic sediments (e.g. Woodside et al. 2003), a velocity of 1,700 m s⁻¹ was chosen to estimate sediment thicknesses and depths derived from the seismic profiles. The chirp signal penetrated 50–75 m below the seabed.

Expanding on earlier CTD (conductivity, temperature, depth)-based datasets acquired during the 2004 Mimes expedition (see “Geological setting” above), the present study reports temperature measurements conducted in the Cheops and Chephren MV brine lakes as well as background measurements in both bottom seawater and sediments at reference sites outside the brine lakes by means of corers launched from aboard ship during the 2007 Medeco2 expedition (for site locations, see Table 2). The background temperature profiles were taken on the flank of the Chephren MV, ~280 m from the MV centre (down to ca. 5 m depth below the seafloor, core MD2-GCT04), and in a seep-free sector of the central Nile province (down to ca. 9 m depth below the seafloor, core MD2-GCT02). Corresponding data were collected at two sites in the Chephren MV brine lake (cores MD2-GCT03 and 05), and one site in the Cheops MV brine lake (core MD2-GCT06).

Temperature measurements were made with Ifremer/Micrel THP thermistor thermometers mounted on outrigger-type probe holders welded to the outer surface of the barrels of 10 m long gravity corers. Up to seven thermometers were used in each case, including one welded to the uppermost part of the corer for measurements at the seawater–sediment or seawater–brine interfaces. A tilt sensor close to the top of the corer served to verify the penetration angle. After penetration into sediments, sufficient time was allocated (usually 10 minutes) for the thermometers to equilibrate to ambient temperatures.

As was to be expected in view of the highly fluidized nature of the brines, the corer cable showed no measurable changes in cable tension during progressive lowering, arguing against firmer stratifications within the brine lakes. The gravity corer was lowered to a maximum depth of 134 and 449 m (relative to the brine lake surface) in the Chephren and Cheops crater lake respectively, at which stage it was decided to terminate the operation for safety reasons. The fluid content of the corer was lost upon core retrieval on board ship, except for the recovery of a ca. 15 cm long silty clay plug in the core catcher of core MD2-GCT06 (Pierre et al. 2014, this volume).

Acoustic water column data were acquired during the 2007 Medeco2 expedition with a single-beam echosounder (EA600, 38 kHz) from aboard the ship. Acoustic gas flares related to fluid venting at the Menes caldera were not identified (although the water column above

the brine lakes was saturated in methane, at least in 2004; Woodside et al. 2004), most likely due to the large water depths.

Assessments of the Cheops and Chephren MVs benefit from high-resolution data acquired during near-bottom multibeam ROV surveys and reported by Dupré et al. (2008a), Foucher et al. (2009) and, in this volume, Mascle et al. (2014) and Pierre et al. (2014). Only selected areas of bathymetric maps are included in this paper.

4. Results

4.1. Multichannel seismic profiles

The high-resolution multichannel seismic profiles display the Plio-Quaternary sediments deposited above the Messinian evaporites (not imaged in Fig. 5). The orientation of the lines, more or less parallel to the listric faults induced by salt tectonics, does not provide evidence for direct fault control of the Menes caldera and the MVs within and outside the caldera. The sedimentary pile is dissected by numerous faults along the two seismic profiles, some of which reach the seafloor (in particular northeast of the Menes caldera, Fig. 5a).

Chaotic reflection zones, most commonly kilometre sized, with various geometries (“Christmas tree” structures, elongated buried lenses) are present along the two profiles, within (Fig. 5a) and outside the Menes caldera (Fig. 5a, b). The Christmas tree identified within the caldera corresponds to a mud volcano associated with subseafloor authigenic carbonates, which was explored in 2003 (Huguen et al. 2009) and 2007, and named Menitites during the Medeco2 expedition (Pierre et al. 2008). The buried chaotic zone identified within the caldera and located northeast of the Menitites MV (between 6.5 and 8.5 km in Fig. 5a) corresponds to irregularities on the seabed (labelled “MV” in Fig. 3a) most likely related to mud expulsion. Similar correlations can be made between the chaotic seismic facies at depth (Fig. 5) and the occurrence of MVs outside the Menes caldera as shown on the bathymetry map (Fig. 2a). These chaotic reflection zones are interpreted to be mud breccia bodies consisting of matrix-supported clast-rich mud bodies typical of erupted material from mud volcanoes. The elongated lenses most likely are mud flows traversed off-axis. The deepest identified mud breccia body is located within the Menes caldera with its base at ~600 m below the seabed (Fig. 5a).

The Christmas tree structure attests to a succession of mud expulsion episodes at the seabed interbedded with normal pelagic sedimentation periods. The Menitites MV, with a ~400 m thick Christmas tree emerging at the seabed as a cone, records at least three major mud expulsion events (Fig. 5a), although upon mud volcano activity destabilized reworked sediments may be emplaced around the mud volcano. The buried Christmas tree outside the Menes caldera appears more disrupted with numerous mud expulsion episodes recorded throughout its ~450 m thickness (Fig. 5b). Both structures are related to long-lasting mud volcanism.

Transparent seismic zones, within and outside the caldera, follow the geometry of the deformed sedimentary layers (e.g. lateral sides of the deepest mud flows of Menitites MV, Fig. 5a), and could correspond to deformed turbiditic lobes of the Nile deep-sea fan, the seismic lines running right across the distal part of the fan (Fig. 1).

The Menes caldera appears as a cone-shaped subsiding structure. Along the SW–NE aligned seismic profiles, only a few faults are observed within the caldera. These are located close to the north-eastern border, where they almost reach the seabed (Fig. 5b).

4.2. Chirp profiles

The high-resolution chirp profiles (Figs. 6 and 7) show the caldera to be a well-developed seafloor depression (see, for example, along the NW–SE MS31ES1 profile, Fig. 6a), and that the active Cheops and Chephren MVs have craters filled with muddy brines, whereas the crater of the inactive Mykerinos MV is empty and the Menitites MV appears as a cone with no brine (cf. Table 1). Mud volcano diameters range from 200 m (unnamed MVs north of Cheops MV; see Fig. 2 in Pierre et al. 2014, this volume) to 1,500 m (Cheops, Chephren and Mykerinos MVs). Their height above the seafloor varies from 10–40 m.

The Mykerinos MV exhibits a deep crater depression which extends ~45 m below its edges (Fig. 6b). As well imaged by high-resolution bathymetry data (Fig. 6e, f), the Chephren and Cheops MVs have relatively flat tops representing the seawater–brine interfaces of the lakes filling the craters (Figs. 6a–c and 7). Variations in the elevation of the brine lake surfaces do not exceed 1 m in both cases. Profiles crossing the centres of the brine lakes, or passing close by, display some strong reflections beneath the lake surface (e.g. Cheops MV, Fig. 6a–c), whereas profiles crossing the edges of the brine lakes (e.g. Chephren MV, Fig. 7) exhibit a chaotic homogenous seismic facies. The strong reflections may be related to the structure of the mud volcanoes or may be caused by changes in mud density, possibly indicating the bottom of the brine lakes. This latter interpretation is also supported by the similarities with the reflections observed at the bottom of the Mykerinos crater where they coincide with the depth of the crater surface (derived from bathymetric data and near-bottom Nautila surveys). In this view, at Cheops MV, the bottom of the brine lake would be at ~10 to 20 m below the seawater–brine interface (Figs. 6a, b and 7). At Chephren MV, the internal reflections of a profile crossing the central part of the brine lake may indicate a depth of 10 m (Fig. 6a).

Within the Menes caldera, both close to the four major MVs and further away from these, the chirp data reveal numerous wipe-outs interpreted as gas-bearing sediments (Figs. 6b, c and 7); some of these are more deeply buried, whereas others are close to the seabed, the sedimentary pile being dissected by numerous small faults (e.g. Fig. 7).

Water column echoes northeast of the Cheops MV (Fig. 6c, d) have the form of low-amplitude diffractions, occurring at either shallower or slightly greater depths than the summit of the MV. These side echoes do not resemble signatures produced by a school of fish or gas bubbles in the water column, the high-resolution bathymetry instead suggesting that they may be caused by the small-scale relief of two small MVs or parasitic cones on Cheops MV (Table 1; see Fig. 2 in Pierre et al. 2014, this volume). Both have a diameter of ~200 m and rise ~20 m above the surrounding seafloor. One of these has an elongated conical shape and is located at the northern foot of the Cheops MV; the other one is more circular and displays a 50 m diameter caldera at the summit. Both MVs are aligned SW–NE, which corresponds to the orientation of the listric faults bordering the southern side of the Menes caldera (Fig. 2).

4.3. Brine and background temperature profiles

In the Chephren MV brine lake, the corer-based temperature profiles recorded in 2007 at two closely spaced sites (MD2-GCT03 and 05, 60 m south of the MV centre, and 30 m distant from each other, Fig. 6e) show very strong increases in temperature with depth ranging from 14.0 °C and 14.1 °C at the seawater–brine interface to ca. 51 °C and 53 °C at 5 m depth below the brine lake surfaces respectively (Fig. 8). The values then continue to increase only slightly to reach ca. 55 °C and 57 °C at 7 m depth respectively. These high temperatures persisted with only minor variations at larger depths, the deepest measurements being at 14 and 134 m for sites MD2-GCT03 and 05 respectively (Figs. 8, 9). Evidence for temperatures consistently levelling off at 57.3–57.5 °C in the 134 m deep profile at site MD2-GCT05 argue

against measurable density layering in deeper brines. The corer cable showed no changes in tension which might have indicated such stratification or the abrupt end of the corer's descent. Small variations ($<1\text{ }^{\circ}\text{C}$) recorded at 45-65 m by only one of the six thermometers can confidently be ignored. These 2007 data for the Chephren brine lake are very similar to the CTD-based measurements carried out in 2004 within 10 m of the MD2-GCT05 site (Fig. 6e), and which showed values levelling off at $57\text{ }^{\circ}\text{C}$ down to 250 m below the seawater-brine interface (as in the present case, that deepest point of measurement was constrained by safety considerations; Woodside et al. 2004; de Lange et al. 2006).

In the Cheops MV brine lake, the 2007 temperature profiles for site MD2-GCT06 located 80 m west of the MV centre (Fig. 6f) exhibit a similar plateauing pattern with increasing brine lake depth, except that the maximum temperature reached was ca. $15\text{ }^{\circ}\text{C}$ cooler than that of the Chephren brine lake. Thus, values increased strongly from $14.1\text{ }^{\circ}\text{C}$ at the seawater-brine interface to plateau at $42.1\pm 1.1\text{ }^{\circ}\text{C}$ from 18 m down to 449 m below the brine lake surface (Figs. 8, 9), depth at which the operation was stopped for safety reasons. The thermal gradient in the shallower brines ($42\text{ }^{\circ}\text{C}/18\text{ m}=2.3\text{ }^{\circ}\text{C m}^{-1}$) is therefore weaker than that of the Chephren brine lake ($57\text{ }^{\circ}\text{C}/7\text{ m}=8.1\text{ }^{\circ}\text{C m}^{-1}$). Five of the seven temperature sensors attached to the corer barrel were functioning in this case, all revealing slight variations in temperature, particularly at 250-300 m below the brine lake surface where values peaked at $43.2\text{ }^{\circ}\text{C}$ (Fig. 9b). Comparative CTD- and corer-based data recorded in 2004 at three closely grouped sites ($<10\text{ m}$) situated 15-20 m northeast of site MD2-GCT06 (cf. Fig. 6f) revealed temperatures reaching 25, 37 and $42\text{ }^{\circ}\text{C}$ at 10 m depth below the brine lake surface, presumably corresponding to the crater lake bottom in this area at that time (Woodside et al. 2004; de Lange et al. 2006).

During the 2007 Medeco2 expedition, background temperatures recorded in subseafloor sediments at reference site MDGCT04, located on the flank of the Chephren MV $\sim 280\text{ m}$ from the MV centre, and reference site MDGCT02 in a seep-free sector of the central Nile province averaged at about $14.1\pm 0.1\text{ }^{\circ}\text{C}$ (Fig. 8). This is very similar to values characterizing the seawater-bottom sediment interface at these sites (Table 2), as well as typical bottom water temperatures in the eastern Mediterranean Sea (cf. Roether et al. 2007).

5. Discussion and conclusions

5.1. Hot brines

Shallow temperatures commonly recorded at the emission centres of active mud volcanoes may reach $40\text{-}50\text{ }^{\circ}\text{C}$ (MacDonald et al. 2000; Dupré et al. 2007; Feseker et al. 2010; Foucher et al. 2010), well above ambient sediment and bottom water temperatures, and even $70\text{ }^{\circ}\text{C}$ (e.g. Kadirov and Mukhtarov 2004; Feseker et al. 2010) and as much as $100\text{ }^{\circ}\text{C}$ in volcanic settings (e.g. Mazzini et al. 2007). Likewise, temperatures in brine-filled craters of mud volcanoes or in deep anoxic basins closely associated with mud volcanism may exceed ambient values by as much as $20\text{-}30\text{ }^{\circ}\text{C}$ (e.g. $48.2\text{ }^{\circ}\text{C}$ in a brine pool in the Gulf of Mexico, MacDonald et al. 2000; $45.3\text{ }^{\circ}\text{C}$ in the Urania Basin, Corselli et al. 1996). In the present study of the Menes caldera in the eastern Mediterranean, the deeper brines of both the Cheops and Chephren brine lakes had temperatures which were (respectively) 28 and $43\text{ }^{\circ}\text{C}$ higher than those of reference sites, and this both in 2004 and 2007. Together with evidence of these high temperatures persisting very stably below the (respectively) 18 and 7 m thick surface layer of the brine lakes, these findings imply good mixing of the muddy brines driven by powerful, ongoing advection of hot fluids from below. Tracking this hot signature down to nearly 0.5 km depth below the brine lake surface arguably sets the current record for such settings worldwide.

The minimum depth from which warm fluids could originate can be roughly estimated considering a seabed temperature of 14 °C and a regional thermal gradient of 16.5 °C km⁻¹. Thermal gradients in a sector free of seepage activity in the central Nile province were 16.4±0.3 °C km⁻¹ (upper 10 m of sediments at site MD2-GCT02, eight thermometers; cf. Table 2 for location). Similar gradients of 16.6±0.1 °C km⁻¹ have been recorded in the eastern Nile province (site MD2-GCT01, 32°36.09'N, 31°20.01'E), and a stronger gradient of 20.0 °C km⁻¹ about 5 km from the active Isis mud volcano (in 2004, site MS22PT; Feseker et al. 2009). Based on these calculations, the fluids emitted at the Chephren and Cheops MVs would originate at 2.6 and 1.7 km below the seabed respectively, which is below the depths of Messinian deposits at these locations, i.e. 1.2-1.6 km (see Fig. 6b in Loncke et al. 2004). These depths are thus consistent with the depth of dissolution of Messinian evaporites and the ages determined for rock clasts from the western Nile province (~35 km from the Menes caldera), which indicate an Early Cretaceous (Berriasian-Valanginian) origin (Giresse et al. 2010).

The temperature in the conduits of mud volcanoes depends on the relative advection rates between gas and mud. Mud is a vector for convective heat transfer, whereas endothermic gas depressuring induces cooling, the effect of cooling being dependent on the local pressure-temperature conditions (e.g. Deville and Guerlais 2009). The inversion of the Joule-Thompson coefficient of methane at 45 °C occurs at 480 bar, and the expansion of pure methane from 370 to 300 bar (from 1.7 km below the seafloor to the seabed) would induce a cooling from 45 to 42 °C (F. Montel, TOTAL, France, personal communication 2014). Plateauing temperature profiles with depth within the brines require a quasi-continuous input of warm fluids and mud to keep large volumes of muddy brines as warm as 57 °C at Chephren MV and 42 °C at Cheops MV against much lower background values of 14 °C (Table 2), and this on a year to year basis. The relatively strong thermal gradients (ca. 8 and 2 °C m⁻¹) recorded in the shallow brine layers (upper 7 and 18 m) of the Chephren and Cheops brine lakes imply that the flow of muddy brines is high and fast enough to inhibit re-equilibration with ambient temperatures. Moreover, the stable temperatures recorded down to 449 and 134 m in 2007 in (respectively) the Cheops and Chephren brine lakes suggest that these depths were still far away from the base of the conduits, where disturbance is expected due to the closer proximity to the gas and mud source (Deville and Guerlais 2009). The 15 °C difference in maximum temperature observed between the two brine lakes may result from a shallower provenance of fluids in the Cheops MV relative to the Chephren MV, or a mixing of cooler fluids at Cheops MV possibly involving downward flows of seawater into the mud volcano. The former hypothesis may be supported by the gas concentrations with regard to the temperatures. In the case of the same source of fluids at the Cheops and Chephren MVs, the higher temperatures at Chephren MV should coincide with lower concentrations of methane as the expansion of gas during ascent would cool the mud, although with a small effect. However, the data do not support this. On the contrary, the warmer Chephren MV records the highest concentration of methane in the brines (Pierre et al. 2008; Table 1) as well as in the water column above (Woodside et al. 2004).

5.2. Salt tectonics and mud volcanism

The 8 km wide Menes caldera (at a depth of 100 m below the surrounding seafloor) is controlled by listric faults related to salt tectonics. A seismic profile oriented NW-SE in Fig. 6 of Loncke et al. (2004) provides evidence of faults rooted in the Messinian evaporites, and converging upwards to the southern and northern limits of the caldera. Growth faults reaching the seabed at the southern limit of the caldera are clearly visible in the bathymetry reported in Figs. 2 and 3 of this paper. The Menes caldera is more or less stable with regard to salt movements, as mobile evaporites are thinned or absent below the caldera. Messinian evaporite-rooted growth faults provide pathways for warm fluids (40-60 °C) to escape from pressurized source levels below the Messinian salt (Loncke et al. 2004; Huguen et al. 2009),

ultimately leading to the formation of mud volcanoes at the seafloor (seven identified so far; Table 1). Seepage activity offshore northern Egypt appears to be a long-lasting phenomenon with initiation of mud volcanism (cf. identification of deeply buried fossil mud bodies within the Pliocene sequence; Fig. 5) in the Early to middle Pliocene, with overpressured shales of Tortonian age as candidates for the mud source (Bentham et al. 2006). Seismic data provide evidence for past and recent mud volcanism widely spread within the 8 km wide Menes caldera and also beyond it, in accordance with the numerous MV structures identified at the seabed (Loncke et al. 2004; Huguen et al. 2009).

5.3. Controls on mud volcano morphology

The Menes caldera hosts three small conical mud volcanoes (e.g. Menitites MV) and four larger mud volcanoes with empty (e.g. Mykerinos MV) or brine-filled (Cheops and Chephren MVs) craters a few hundreds of metres in diameter (Table 1). Variations in MV morphology may be due to complex interrelationships between driving force (pressure), conduit width and material supply, or they could represent different stages of MV evolution (Lance et al. 1998; Kopf 2002; Yusifov and Rabinowitz 2004). The smaller conical MVs of the Menes caldera are not associated with brine seepage, their mud breccias obviously having a much higher viscosity than the muddy brines. The lower viscosity of muddy brines within wide depressions such as the craters at the summits of the Chephren and Cheops MVs results in the formation of brine lakes with a very flat seawater-brine interface associated with a very strong density contrast. For example, the 310 PSU brine of the Chephren lake has a density of 1.200 g cm^{-3} , well above the 1.028 g cm^{-3} of typical Mediterranean seawater.

It is commonly thought that the depressions or craters which may develop at MV summits result from subsidence caused by the loss of fluids and sediments during eruptions, followed by a phase of continued extrusive activity (Deville et al. 2006; Evans et al. 2008). Subsidence is generally of the order of several tens of metres (e.g. Kopf et al. 1998). The formation of chambers of liquefied mud at relatively shallow depths above the zone of overpressure has been proposed as a key component of mud volcanism (Deville et al. 2003, 2006). As expulsion of mud continues, the depletion of the reservoir at depth causes the central area to sink and eventually collapse. Subsidence commonly occurs along a series of normal faults dipping towards the centre of the mud volcano. This scenario has been invoked for the development of numerous calderas (e.g. Bonini 2008; Praeg et al. 2009). The craters at the summits of the four MVs of the Menes caldera may therefore have been created by the same mechanism, the subsidence following depletion of the mud chambers (although no seismic data are available to the vertical of the MVs that could image these mud chambers) producing the faults around the MVs identified in the chirp profiles of the present study.

5.4. Feeder channel geometry

The 250 m width of the Cheops and Chephren brine lakes can be confidently inferred from near-bottom high-resolution multibeam surveys and visual observations (Table 1). Moreover, deployment of corers and CTDs to large depths reaching, for example, ca. 0.5 km below the seawater-brine interface of the Cheops MV can plausibly be explained by the presence of a feeder channel.

Consistent with width/depth ratios ranging from 10 to 50 for brine depressions in other world regions (Table 3), the average depth of the brine lakes at the Cheops and Chephren MVs would be a few tens of metres relative to the seawater-brine interface. Indeed, the chirp profiles support this interpretation, revealing the presence of strong hyperbolic intersections at such depths below the brine lake surface, unless these echoes correspond to a density contrast between an upper mixing layer and a homogenous high-temperature brine below.

Moreover, the lowering of a CTD into the Cheops MV brine lake in 2004 reached only 10 m, possibly corresponding to the bottom of the brine lake, unless the neck of the mud volcano was full of denser mud at that time (see “Results” above). It is also worth noting that Mykerinos MV, most likely a former brine lake (Gontharet et al. 2007; Huguen et al. 2009), has a 45 m deep “empty” crater today. Although this depth would not precisely correspond to that of the former brine lake, due to subsequent crater infilling and subsidence after the cessation of brine seepage, it does provide an order of magnitude. Similarly, the empty crater at the summit of the mud volcano located just south of Chephren MV (Table 1; Foucher et al. 2009; Mascle et al. 2014, this volume), also interpreted to be a former brine lake, has a present-day depth of 20 m.

It is generally considered that feeder channels of MVs are narrow (van Rensbergen et al. 1999; Stewart and Davies 2006; Dupré et al. 2007), although some MVs may be underlain by wider seismically defined gas chimneys. Larger features are generally thought to have wider conduits (Kopf 2002). Despite the limited number of corer/CTD deployments, the strong similarity in the temperature profiles between 2004 and 2007 suggest that, at both brine lakes, lowerings of the instruments distant by a few tens of metres correspond to the same conduit. In the Chephren brine lake in 2004 and 2007, successful corer/CTD deployments to large depths (134 and 250 m below the lake surface) at two closely spaced sites (within a few tens of metres of each other) suggest the persistence of one and the same feeder channel in this area, which would therefore be at least a few tens of metres wide. This is consistent with the similarity of the temperature profiles from the two sites-in deeper brines, values plateau at 55-57 °C in all cases. Interestingly, this feeder channel is not located at the geometric centre of the MV but is distinctly offset to the south, similarly to the offset of the crater relative to the overall structure at the MV located south of it (Table 1, see Fig. 4b in Mascle et al. 2014, this volume). Likewise, the feeder channel traced to a depth of ca. 0.5 km in the Cheops crater lake is located southwest of the geometric centre (Fig. 6e, f). These findings are consistent with a lateral migration of feeder channels in the course of time (Fig. 10). Former and active brine lakes provide also support for lateral migration of fluid pathways. The two mud volcanoes of similar size, one with an empty depression, the other with a brine-filled depression (Chephren MV), would account for a lateral migration of the main feeding conduit by 250 m, at least in the upper part of the system. Unlike logistically less challenging settings such as mud pools of onshore mud volcanoes (e.g. Deville and Guerlais 2009), exploring the more detailed geometry of these submarine feeder channels (e.g. only one main feeder channel as opposed to a dense network of narrower channels?) is a daunting task which deserves further attention.

Within this context, it cannot be excluded that, in the vicinity of the Menes caldera, seabed seepage may also occur away from the mud volcanoes. This would be consistent with the presence of buried mud bodies within and outside the caldera throughout the Pliocene sequence. Furthermore, some of the faults identified along the chirp profiles are connected to gas-saturated sediments (acoustic wipe-out zones). Those intersecting the seafloor could provide conduits for seafloor emissions, thus marking potential sites of future mud volcano and brine lake development.

In conclusion, Fig. 10 conceptualizes the functioning and evolution of mud volcanoes characterized by ongoing and earlier brine seepage in the Menes caldera. The MVs are the seabed expression of deep thermogenic processes involving the dissolution of Messinian evaporites by warm fluids likely sourced at even greater depths-e.g. 2.6 and 1.7 km below the seabed at the active Chephren and Cheops MVs respectively. Deeply rooted fluid conduits, possibly a few tens of metres wide, are revealed by temperatures as high as 42 and 57 °C tracked down to nearly (respectively) 0.5 and 0.25 km depth below the brine lake surface at the Cheops and Chephren MVs.

Sampling and in situ physicochemical measurements have proven challenging in the brine crater lakes of the deep-water mud volcanoes of the Menes caldera. Future research should aim at a denser network of corer and CTD deployments, together with multi-parameter sensors to derive, for example, vertically well resolved density profiles. These datasets should be collected concurrently to minimize potentially confounding effects of strong short-term and small-scale variability characterizing this highly dynamic environment.

Acknowledgements

We are grateful to the officers and crews of the *R/V Pelagia* and *R/V Pourquoi pas?* for the successful operations conducted during the Mimes and Medeco2 expeditions respectively. Alain Moreau provided the processed multichannel seismic profiles. We would like to thank Anne Pacault for her assistance in chirp data acquisition and processing, and Laëticia Brosolo for processing the high-resolution bathymetry maps. Also acknowledged are valuable suggestions and improvements from Patrice Imbert, an anonymous reviewer, as well as the journal editors. MIMES was a part of MEDIFLUX, a cooperative Dutch-French-German programme endorsed and promoted by the European Science Foundation within its EUROMARGINS initiative (contract no. ERAS-CT-2003-980409 of the European Commission, DG Research, FP6). The Netherlands Organisation for Scientific Research (NWO) is thanked for the Dutch financial support within MEDIFLUX through NWO/ALW project 855.01.031. The MEDECO2 cruise was supported and processed thanks to HERMES (EC contract no. GOCE-CT-2005-511234) and HERMIONE (EC contract no. FP7-ENV-2008-1-226354) programmes, funded by the European Commission's Framework Six and Seven programmes.

References

- Aal AA, El Barkooky A, Gerrits M, Meyer HJ, Schwander M, Zaki H (2001) Tectonic evolution of the eastern Mediterranean Basin and its significance for the hydrocarbon prospectivity of the Nile Delta deepwater area. *GeoArabia* (Manama) 6(3):363–384
- Aiello IW, Zabel M, Hinrichs K-U, Teske A, Goldhammer T, Elvert M, Heuer S (2012) An expanded seafloor in the brine lake of Urania Basin: a new deep-water marine environment. In: *Abstr Vol 11th Int Conf Gas in Marine Sediments*, 4–7 September 2012, Nice, France, pp 18–19
- Bayon G, Loncke L, Dupré S, Caprais JC, Ducassou E, Duperron S, Etoubleau J, Foucher JP, Fouquet Y, Gontharet S, Henderson GM, Huguen C, Klaucke I, Mascle J, Migeon S, Olu-Le Roy K, Ondréas H, Pierre C, Sibuet M, Stadnitskaia A, Woodside J (2009) Multi-disciplinary investigation of fluid seepage on an unstable margin: the case of the Central Nile deep sea fan. *Mar Geol* 261(1/4):92–104
- Bayon G, Dupré S, Ponzevera E, Etoubleau J, Cheron S, Pierre C, Mascle J, Boetius A, de Lange GJ (2013) Formation of carbonate chimneys in the Mediterranean Sea linked to deep-water oxygen depletion. *Nature Geosci* 6:755–760. doi:10.1038/ngeo1888
- Bellaiche G, Loncke L, Gaullier V, Mascle J, Courp T, Moreau A, Radan S, Sardou O (2001) Le cône sous-marin du Nil et son réseau de chenaux profonds; nouveaux résultats (campagne Fanil). *C R Acad Sci II Sci Terre Planètes* 333(7):399–404
- Bentham P, Pasley M, Birt C (2006) The style and timing of mud volcanism in the offshore Nile Delta, Egypt. In: *Abstr Vol AAPG/GSTT Hedberg Conf Mobile Shale Basins - Genesis, Evolution and Hydrocarbon Systems*, 4–7 June 2006, Port of Spain, Trinidad & Tobago

- Bernard B, Potter J, Brooks J, Shedd W, Petersen C, Bright M, Goehring L, Cordes E, Hourdez S, Hunt J Jr, Kupchik M, Becker E, Joye S, Bowles M, Carney R, Fisher C, Nelson K, Boland G, Samarkin V, Bernier M, Telesnicki G, Lessard-Pilon S, MacDonald I, Niemann H (2007) Alvin explores the deep Northern Gulf of Mexico slope. *Eos Trans Am Geophys Union* 88:35. doi:10.1029/2007EO350001
- Bonini M (2008) Elliptical mud volcano caldera as stress indicator in an active compressional setting (Nirano, Pedemontane margin, northern Italy). *Geology* 36(2):131–134. doi:10.1130/G24158A.1
- Borin S, Brusetti L, Mapelli F, D'Auria G, Brusa T, Marzorati M, Rizzi A, Yakimov M, Marty D, de Lange GJ, Van der Wielen P, Bolhuis H, McGenity TJ, Polymenakou PN, Malinverno E, Giuliano L, Corselli C, Daffonchio D (2009) Sulfur cycling and methanogenesis primarily drive microbial colonization of the highly sulfidic Urania deep hypersaline basin. *Proc Natl Acad Sci USA* 106(23):9151–9156. doi:10.1073/pnas.0811984106
- Bourry C, Chazallon B, Charlou JL, Pierre Donval J, Ruffine L, Henry P, Geli L, Çagatay MN, Inan S, Moreau M (2009) Free gas and gas hydrates from the Sea of Marmara, Turkey: chemical and structural characterization. *Chem Geol* 264(1/4):197–206
- Caméra L, Ribodetti A, Mascle J (2010) Deep structures and seismic stratigraphy of the Egyptian continental margin from multichannel seismic data. *Geol Soc Lond Spec Publ* 341(1):85–97. doi:10.1144/SP341.5
- Camerlenghi A, Cita MB, Hieke W, Ricchiuto T (1992) Geological evidence for mud diapirism on the Mediterranean Ridge accretionary complex. *Earth Planet Sci Lett* 109(3/4):493–504. doi:10.1016/0012-821x(92)90109-9
- Capozzi R, Picotti V (2002) Fluid migration and origin of a mud volcano in the Northern Apennines (Italy); the role of deeply rooted normal faults. *Terra Nova* 14(5):363–370
- Charlou JL, Donval JP, Zitter T, Roy N, Jean-Baptiste P, Foucher JP, Woodside JM (2003) Evidence of methane venting and geochemistry of brines on mud volcanoes of the eastern Mediterranean Sea. *Deep Sea Res I Oceanogr Res Papers* 50(8):941–958
- Cita MB (2006) Exhumation of Messinian evaporites in the deep-sea and creation of deep anoxic brine-filled collapsed basins. *Sediment Geol* 188:357–378. doi:10.1016/j.sedgeo.2006.03.013
- Cita MB, Ryan WBF, Paggi L (1981) Prometheus mud breccia; an example of shale diapirism in the Western Mediterranean Ridge. *Ann Géol Pays Héliéniques* 30:543–570
- Corselli C, Basso D, de Lange G, Thomson J (1996) Mediterranean Ridge Accretionary Complex yields rich surprises. *Eos Trans Am Geophys Union* 77(24):227–227. doi:10.1029/96EO00159
- Davies RJ, Stewart SA (2005) Emplacement of giant mud volcanoes in the south Caspian Basin; 3D seismic reflection imaging of their root zones. *J Geol Soc Lond* 162(1):1–4
- de Lange GJ, Boelrijk N, Catalano G, Corselli C, Klinkhammer GP, Middelburg JJ, Muller DW, Ullman WJ, Vangaans P, Woittiez JRW (1990) Sulfate-related equilibria in the hypersaline brines of the Tyro and Bannock Basins, eastern Mediterranean. *Mar Chem* 31(1/3):89–112. doi:10.1016/s0304-4203(05)80006-4
- de Lange G, Mastalerz V, Dählmann A, Haese R, Mascle J, Woodside JM, Foucher J-P, Lykousis V, Michard A (2006) Geochemical composition and origin for fluid and gas fluxes at Eastern Mediterranean mud volcanoes. In: *CIESM Worksh Monogr Fluids seepages / mud volcanism in the Mediterranean and adjacent domains*, vol 29, pp 103–110
- Deville E, Guerlais SH (2009) Cyclic activity of mud volcanoes: evidences from Trinidad (SE Caribbean). *Mar Petrol Geol* 26(9):1681–1691
- Deville E, Battani A, Gribouard R, Guerlais S, Herbin JP, Houzay JP, Muller C, Prinzhofer A (2003) The origin and processes of mud volcanism; new insights from Trinidad. *Geol Soc Spec Publ* 216:475–490
- Deville E, Guerlais S-H, Callec Y, Gribouard R, Huyghe P, Lallemand S, Mascle A, Noble M, Schmitz J (2006) Liquefied vs stratified sediment mobilization processes: insight from the south of the Barbados accretionary prism. *Tectonophysics* 428(1/4):33–47

- Dimitrov L, Woodside J (2003) Deep sea pockmark environments in the eastern Mediterranean. *Mar Geol* 195(1/4):263–276
- Dolson JC, Shann MV, Matbouly S, Harwood C, Rashed R, Hammouda H (2001) The petroleum potential of Egypt. *AAPG Memoir* 74:453–482
- Dolson JC, Boucher PJ, Dodd T, Ismail J (2002) Petroleum potential of an emerging giant gas province, Nile Delta and Mediterranean Sea off Egypt. *Oil Gas J* 100(20):32–37
- Duperron S, Halary S, Lorion J, Sibuet M, Gail F (2008) Unexpected co-occurrence of six bacterial symbionts in the gills of the cold seep mussel *Idas* sp. (Bivalvia: Mytilidae). *Environ Microbiol* 10:433–445
- Dupré S, Woodside J, Foucher J-P, de Lange G, Mascle J, Boetius A, Mastalerz V, Stadnitskaia A, Ondréas H, Huguen C, Harmegnies F, Gontharet S, Loncke L, Deville E, Niemann H, Omorieg E, Olu-Le Roy K, Fiala-Medioni A, Dählmann A, Caprais J-C, Prinzhofer A, Sibuet M, Pierre C, Sinninghe Damsté J, NAUTINIL scientific party (2007) Seafloor geological studies above active gas chimneys off Egypt (Central Nile Deep Sea Fan). *Deep Sea Res I Oceanogr Res Papers* 54(7):1146–1172
- Dupré S, Brosolo L, Mascle J, Pierre C, Harmegnies F, Mastalerz V, Bayon G, Ducassou E, De Lange G, Foucher J-P, the Victor ROV Team, the Medeco Leg 2 Scientific Party (2008a) The Menes mud volcano caldera complex: an exceptional site of brine seepage in the deep waters off north-western Egypt. In: *Abstr Vol 9th Int Conf Gas in Marine Sediments*, 15–19 September 2008, Bremen, Germany, pp 21–22
- Dupré S, Buffet G, Mascle J, Foucher J-P, Gauger S, Boetius A, Marfia C, the AsterX AUV Team, the Quest ROV Team, the BIONIL Scientific Party (2008b) High-resolution mapping of large gas emitting mud volcanoes on the Egyptian continental margin (Nile Deep Sea Fan) by AUV surveys. *Mar Geophys Res* 29(4):275–290
- Dupré S, Woodside J, Klaucke I, Mascle J, Foucher J-P (2010) Widespread active seepage activity on the Nile Deep Sea Fan (offshore Egypt) revealed by high-definition geophysical imagery. *Mar Geol* 275(1/4):1–19
- Evans RJ, Stewart SA, Davies RJ (2008) The structure and formation of mud volcano summit calderas. *J Geol Soc* 165:769–780. doi:10.1144/0016-76492007-118
- Feseker T, Dählmann A, Foucher JP, Harmegnies F (2009) In-situ sediment temperature measurements and geochemical porewater data suggest highly dynamic fluid flow at Isis mud volcano, eastern Mediterranean Sea. *Mar Geol* 261(1/4):128–137
- Feseker T, Brown KR, Blanchet C, Scholz F, Nuzzo M, Reitz A, Schmidt M, Hensen C (2010) Active mud volcanoes on the upper slope of the western Nile deep-sea fan—first results from the P362/2 cruise of R/V *Poseidon*. *Geo-Mar Lett* 30:169–186. doi:10.1007/s00367-010-0192-0
- Foucher J-P, Westbrook GK, Boetius A, Ceramicola S, Dupré S, Mascle J, Mienert J, Pfannkuche O, Pierre C, Praeg D (2009) Structure and drivers of hydrocarbon seep ecosystems in the European seas: an overview from HERMES results. *Oceanography* 22(1):92–109
- Foucher J-P, Dupré S, Scalabrin C, Feseker T, Harmegnies F, Nouzé H (2010) Changes in seabed morphology, mud temperature and free gas venting at the Håkon Mosby mud volcano, offshore northern Norway, over the time period 2003–2006. *Geo-Mar Lett* 30:157–167. doi:10.1007/s00367-010-0193-7
- Gaullier V, Mart Y, Bellaiche G, Mascle J, Vendeville BC, Zitter T, Benkheilil J, Buffet G, Droz L, Ergun M, Huguen C, Kopf A, Levy R, Limnov A, Shaked Y, Volkonskaia A, Woodside JM, Prismed II Second Leg Scientific Party France (2000) Salt tectonics in and around the Nile deep-sea fan; insights from the PRISMED II cruise. *Geol Soc Spec Publ* 174:111–129
- Gay A, Lopez M, Berndt C, Séranne M (2007) Geological controls on focused fluid flow associated with seafloor seeps in the Lower Congo Basin. *Mar Geol* 244(1/4):68–92
- Giresse P, Loncke L, Huguen C, Muller C, Mascle J (2010) Nature and origin of sedimentary clasts associated with mud volcanoes in the Nile deep-sea fan. Relationships with fluid venting. *Sediment Geol* 228(3/4):229–245. doi:10.1016/j.sedgeo.2010.04.014

- Gontharet S, Pierre C, Blanc-Valleron MM, Rouchy JM, Fouquet Y, Bayon G, Foucher JP, Woodside J, Mascle J (2007) Nature and origin of diagenetic carbonate crusts and concretions from mud volcanoes and pockmarks of the Nile deep-sea fan (eastern Mediterranean Sea). *Deep Sea Res II Topical Studies Oceanogr* 54(11/13):1292–1311
- Hartmann M, Scholten JC, Stoffers P, Wehner F (1998) Hydrographic structure of brine-filled deeps in the Red Sea—new results from the Shaban, Kebrit, Atlantis II, and Discovery Deep. *Mar Geol* 144(4):311–330. doi:10.1016/S0025-3227(97)00055-8
- Ho S, Cartwright JA, Imbert P (2012) Vertical evolution of fluid venting structures in relation to gas flux, in the Neogene-Quaternary of the Lower Congo Basin, Offshore Angola. *Mar Geol* 332/334:40–55. doi:10.1016/j.margeo.2012.08.011
- Hsü KJ, Cita MB, Ryan WBF (1973) The origin of the Mediterranean evaporites. In: *Initial Reports Deep Sea Drilling Project 13, Part 2*, pp 1203–1231, College Station, TX
- Huguen C, Mascle J, Woodside J, Zitter T, Foucher JP (2005) Mud volcanoes and mud domes of the Central Mediterranean Ridge: near-bottom and in situ observations. *Deep Sea Res I Oceanogr Res Papers* 52(10):1911–1931
- Huguen C, Foucher JP, Mascle J, Ondréas H, Thouement M, Gontharet S, Stadnitskaia A, Pierre C, Bayon G, Loncke L, Boetius A, Bouloubassi I, de Lange G, Caprais JC, Fouquet Y, Woodside J, Dupré S (2009) Menes caldera, a highly active site of brine seepage in the Eastern Mediterranean sea: “in situ” observations from the NAUTINIL expedition (2003). *Mar Geol* 261(1/4):138–152
- Joye SB, MacDonald IR, Montoya JP, Peccini M (2005) Geophysical and geochemical signatures of Gulf of Mexico seafloor brines. *Biogeosciences* 2:295–309. doi:10.5194/bg-2-295-2005
- Joye SB, Samarkin VA, Orcutt BN, MacDonald IR, Hinrichs K-U, Elvert M, Teske AP, Lloyd KG, Lever MA, Montoya JP, Meile CD (2009) Metabolic variability in seafloor brines revealed by carbon and sulphur dynamics. *Nature Geosci* 2:349–354. doi:10.1038/ngeo475
- Judd AG, Hovland M (2007) *Seabed fluid flow. The impact on geology, biology and the marine environment*. Cambridge University Press, Cambridge
- Kadirov FA, Mukhtarov AS (2004) Geophysical fields, deep structure, and dynamics of the Lokbatan mud volcano. *Russian Acad Sci Phys Solid Earth* 40(4):327–333
- Kopf AJ (2002) Significance of mud volcanism. *Rev Geophys* 40(2):2-1–2-52. doi:10.1029/2000RG000093
- Kopf A, Robertson AHF, Clennell MB, Flecker R (1998) Mechanisms of mud extrusion on the Mediterranean Ridge Accretionary Complex. *Geo-Mar Lett* 18:97–114. doi:10.1007/s003670050058
- Lance S, Henry P, Le Pichon X, Lallemand S, Chamley H, Rostek F, Faugères J-C, Gonthier E, Olu K (1998) Submersible study of mud volcanoes seaward of the Barbados accretionary wedge: sedimentology, structure and rheology. *Mar Geol* 145(3/4):255–292. doi:10.1016/S0025-3227(97)00117-5
- Langseth MG, Westbrook GK, Hobart MA (1988) Geophysical survey of a mud volcano seaward of the Barbados Ridge Accretionary Complex. *J Geophys Res* 93:1049–1061
- Loncke L (2002) *Le delta profond du Nil: structure et évolution depuis le Messinien*. Thèse de doctorat, Université Pierre et Marie Curie, Paris
- Loncke L, Mascle J, Fanil Scientific Parties (2004) Mud volcanoes, gas chimneys, pockmarks and mounds in the Nile deep-sea fan (eastern Mediterranean); geophysical evidences. *Mar Petrol Geol* 21(6):669–689
- Loncke L, Gaullier V, Mascle J, Vendeville B, Camera L (2006) The Nile deep-sea fan: an example of interacting sedimentation, salt tectonics, and inherited subsalt paleotopographic features. *Mar Petrol Geol* 23(3):297–315
- MacDonald IR, Reilly JF, Guinasso NL, Brooks JM, Carney RS, Bryant WA, Bright TJ (1990) Chemosynthetic mussels at a brine-filled pockmark in the Northern Gulf of Mexico. *Science* 248(4959):1096–1099. doi:10.1126/science.248.4959.1096

- MacDonald IR, Buthman DB, Sager WW, Peccini MB, Guinasso NL (2000) Pulsed oil discharge from a mud volcano. *Geology* 28(10):907–910. doi:10.1130/0091-7613(2000)28<907:podfam>2.0.co;2
- Masclé J, Mary F, Praeg D, Brosolo L, Camera L, Ceramicola S, Dupré S (2014) Distribution and geological control of mud volcanoes and other fluid/free gas seepage features in the Mediterranean Sea and nearby Gulf of Cadix. *Geo-Mar Lett* 34. doi:10.1007/s00367-014-0356-4
- Mazzini A, Svensen H, Akhmanov GG, Aloisi G, Planke S, Mathe-Sørensen A, Istadi B (2007) Triggering and dynamic evolution of the LUSI mud volcano, Indonesia. *Earth Planet Sci Lett* 261(3/4):375–388
- Neurauter TW, Roberts HH (1994) Three generations of mud volcanoes on the Louisiana continental slope. *Geo-Mar Lett* 14:120–125. doi:10.1007/BF01203723
- Nuzzo M, Elvert M, Schmidt M, Scholz F, Reitz A, Hinrichs K-U, Hensen C (2012) Impact of hot fluid advection on hydrocarbon gas production and seepage in mud volcano sediments of thick Cenozoic deltas. *Earth Planet Sci Lett* 341/344:139–157. doi:10.1016/j.epsl.2012.05.009
- Omereglio EO, Mastalerz V, de Lange G, Straub KL, Kappler A, Røy H, Stadnitskaia A, Foucher J-P, Boetius A (2008) Biogeochemistry and community composition of iron- and sulfur-precipitating microbial mats at the Chefren mud volcano (Nile Deep Sea Fan, Eastern Mediterranean). *Appl Environ Microbiol* 74(10):3198–3215. doi:10.1128/AEM.01751-07
- Paull CK, Ussler W III, Holbrook WS, Hill TM, Keaten R, Mienert J, Hafliðason H, Johnson JE, Winters WJ, Lorenson TD (2008) Origin of pockmarks and chimney structures on the flanks of the Storegga Slide, offshore Norway. *Geo-Mar Lett* 28:43–51. doi:10.1007/s00367-007-0088-9
- Pautot G, Guennoc P, Coutelle A, Lyberis N (1984) Discovery of a large brine deep in the northern Red Sea. *Nature* 310:133–136. doi:10.1038/310133a0
- Pierre C, Masclé J, Dupré S (2008) MEDECO Leg 2 cruise report. R/V Pourquoi pas? 02 to 30 November 2007 Rhodes-Toulon. Ifremer, Plouzané. <http://archimer.ifremer.fr/doc/00134/24550/>
- Pierre C, Bayon G, Blanc-Valleron M-M, Masclé J, Dupré S (2014) Authigenic carbonates related to active seepage of methane-rich hot brines at the Cheops mud volcano, Menes caldera (Nile deep-sea fan, eastern Mediterranean Sea). *Geo-Mar Lett* 34. doi:10.1007/s00367-014-0362-6
- Pilcher RS, Blumstein RD (2007) Brine volume and salt dissolution rates in Orca Basin, northeast Gulf of Mexico. *AAPG Bull* 91(6):823–833. doi:10.1306/12180606049
- Praeg D, Ceramicola S, Barbieri R, Unnithan V, Wardell N (2009) Tectonically-driven mud volcanism since the late Pliocene on the Calabrian accretionary prism, central Mediterranean Sea. *Mar Petrol Geol* 26(9):1849–1865. doi:10.1016/j.marpetgeo.2009.03.008
- Prinzhofer A, Deville E (2013) Origins of hydrocarbon gas seeping out from offshore mud volcanoes in the Nile delta. *Tectonophysics* 591:52–61
- Robertson AHF, Emeis KC, Richter C, Blanc VMM, Bouloubassi I et al. (1996) Mud volcanism on the Mediterranean Ridge. In: Emeis KC, Robertson AHF, Richter C et al. (eds) *Mediterranean I, Leg 160, cruises of the drilling vessel JOIDES Resolution, Las Palmas, Gran Canaria, to Naples, Italy, Sites 963-973, 7 March-3 May, 1995. Proc Ocean Drilling Program, Part A: Initial Reports, vol 160. Texas A&M University, College Station, TX, pp 521–526*
- Roether W, Klein B, Manca BB, Theocharis A, Kioroglou S (2007) Transient Eastern Mediterranean deep waters in response to the massive dense-water output of the Aegean Sea in the 1990s. *Progr Oceanogr* 74(4):540–571. doi:10.1016/j.pocean.2007.03.001
- Sager WW, MacDonald IR, Hou R (2003) Geophysical signatures of mud mounds at hydrocarbon seeps on the Louisiana continental slope, northern Gulf of Mexico. *Mar Geol* 198(1/2):97–132

- Sardou O, Mascle J (2003) Cartography by multibeam echo-sounder of the Nile deep-sea Fan and surrounding areas (2 sheets). Special publication CIESM, Monaco
- Shokes RF, Trabant PK, Presley BJ, Reid DF (1977) Anoxic, hypersaline basin in the Northern Gulf of Mexico. *Science* 196(4297):1443–1446. doi:10.1126/science.196.4297.1443
- Stewart SA, Davies RJ (2006) Structure and emplacement of mud volcano systems in the South Caspian Basin. *AAPG Bull* 90(5):771–786
- Vandré C, Cramer B, Gerling P, Winsemann J (2007) Natural gas formation in the western Nile delta (Eastern Mediterranean): thermogenic versus microbial. *Org Geochem* 38(4):523–539
- van Rensbergen P, Morley CK, Ang DW, Hoan TQ, Lam NT (1999) Structural evolution of shale diapirs from reactive rise to mud volcanism; 3D seismic data from the Baram Delta, offshore Brunei Darussalam. *J Geol Soc Lond* 156(3):633–650
- van Rensbergen P, Rabaut A, Colpaert A, Ghislain TS, Mathijs M, Bruggeman A (2007) Fluid migration and fluid seepage in the Connemara Field, Porcupine Basin interpreted from industrial 3D seismic and well data combined with high-resolution site survey data. *Int J Earth Sci* 96(1):185–197
- Whiticar MJ (1999) Carbon and hydrogen isotope systematics of bacterial formation and oxidation of methane. *Chem Geol* 161(1/3):291–314. doi:10.1016/S0009-2541(99)00092-3
- Wiedicke M, Neben S, Spiess V (2001) Mud volcanoes at the front of the Makran accretionary complex, Pakistan. *Mar Geol* 172(1/2):57–73
- Woodside JM, Volgin AV (1996) Brine pools associated with Mediterranean Ridge mud diapirs: an interpretation of echo-free patches in deep tow sidescan sonar data. *Mar Geol* 132(1/4):55–61
- Woodside JM, Modin DI, Ivanov MK (2003) An enigmatic strong reflector on subbottom profiler records from the Black Sea—the top of shallow gas hydrate deposits. *Geo-Mar Lett* 23:269–277. doi:10.1007/s00367-003-0149-7
- Woodside JM, de Lange G, Dupré S (2004) Mimes (Multiscale Investigations of Eastern Mediterranean Seep Systems). An expedition on Pelagia 13 June 2004 - 14 July 2004: a contribution to the Mediflux projet of Euromargins. Cruise report, Ifremer, Plouzané. <http://archimer.ifremer.fr/doc/00175/28649/>
- Yusifov M, Rabinowitz PD (2004) Classification of mud volcanoes in the South Caspian Basin, offshore Azerbaijan. *Mar Petrol Geol* 21(8):965–975
- Zitter TAC, Huguen C, ten Veen J, Woodside JM (2006) Tectonic control on mud volcanoes and fluid seeps in the Anaximander Mountains, eastern Mediterranean Sea. *Geol Soc Am Spec Papers* 409:615–631. doi:10.1130/2006.2409(28)

Tables

Table 1 Morphological characteristics of the seven known MVs in the Menes caldera, and chemical brine signatures for the Cheops and Chephren MV craters (*abs* above seafloor). The morphological characteristics are derived from bathymetry (Figs. 3, 6e, f; Sardou and Mascle 2003; Foucher et al. 2009; Mascle et al. 2014; Pierre et al. 2014, this volume), chirp profiles (Figs. 6, 7) and in situ observations (Huguen et al. 2009)

	Cheops	Chephren	MV south of Chephren	Mykerinos	Menitites	Small MVs	
Latitude	32°08.18' N	32°06.57' N	32°06.39' N	32°07.33' N	32°08.44' N	32°08.48' N	32°08.42' N
Longitude	28°09.48' E	28°10.65' E	28°10.67' E	28°11.61' E	28°08.38' E	28°09.66' E	28°09.53' E
Water depth at MV base (m)	3,005–3,010	2,990–3,015	2,990–3,015	2,980–3,000	3,005–3,015	3,010–3,015	3,000–3,010
Diameter (m)	1,500	1,500	1,500	1,500	400	200	200
Height (m asf)	25	40	40	10	30	20	20
Crater-like depressions							
Present day	Muddy brine lake	Muddy brine lake	Former brine lake?	Former brine lake	None	Caldera	None
Diameter (m)	250	250	250	750	-	50	-
Crater depth (m)	Few tens of m	Few tens of m	20	45	-	4	-
<i>Salinity</i> (PSU): 2003 (Huguen et al. 2009): Cheops, 130–310; Chephren, 89–153. 2004 (de Lange et al. 2006): Cheops, 300; Chephren, 150. 2007 (Pierre et al. 2008, 2014 in this volume): Cheops, 210–244							
<i>H₂S</i> (mmol l ⁻¹): Huguen et al. (2009): Cheops, 0.2; Chephren, 0.5–7.2							
<i>CH₄</i> (mmol l ⁻¹): 2003 (Huguen et al. 2009): Cheops, 0.1–2.9; Chephren, 0.6–2.5. 2007 (Pierre et al. 2008, 2014 in this volume): Cheops, 2.4–3.7; Chephren, 0.4–5.6							
<i>Sulphate</i> (mmol l ⁻¹): Huguen et al. (2009): Cheops, 15–24; Chephren, 33–57							

Table 2 Temperatures (mean±standard deviation) at the seawater–brine interface of the Chephren and Cheops brine lakes and at the seawater–bottom sediment interface at reference sites investigated during the 2007 Medeco2 expedition (cf. Figs. 8 and 9; NDSF seep-free background site, central province of Nile deep-sea fan)

Site	Core	Latitude	Longitude	Water depth (m)	Temperature (°C)
Seep-free NDSF	MD2-GCT02	32°34.64'N	29°38.06'E	2,220	14.0066±0.0001 ^a
Chephren brine lake	MD2-GCT03	32°06.52'N	28°10.68'E	2,964	13.9787±0.0024 ^b
Flank of Chephren MV	MD2-GCT04	32°06.49'N	28°10.51'E	2,966	14.0434±0.0006 ^a
Chephren brine lake	MD2-GCT05	32°06.52'N	28°10.66'E	2,961	14.0659±0.0093 ^b
Cheops brine lake	MD2-GCT06	32°08.15'N	28°09.44'E	2,987	14.0584±0.0024 ^b

^aMean measured seawater temperature based on 25 measurements over a few minutes

^bMean calculated seawater temperature based on 25 measurements per thermometer (seven) over a few minutes

Table 3 Width and depth of brine basins, lakes and pools in the eastern Mediterranean (E. Med.) and the Gulf of Mexico (GoM)

	Width	Depth of brine
Deep anoxic basins, E. Med. (Cita 2006)	Several km	100–500 m
Nadir brine lake, E. Med. (Charlou et al. 2003)	250 m	15 m
AC601 brine lake, GoM (Bernard et al. 2007)	180 m	4 m
GB233 brine lake, GoM (MacDonald et al. 2000)	50 m	0.7–3.2 m
Napoli brine pools, E. Med. (Huguen et al. 2005)	Few tens of m	Few tens of cm

Figures

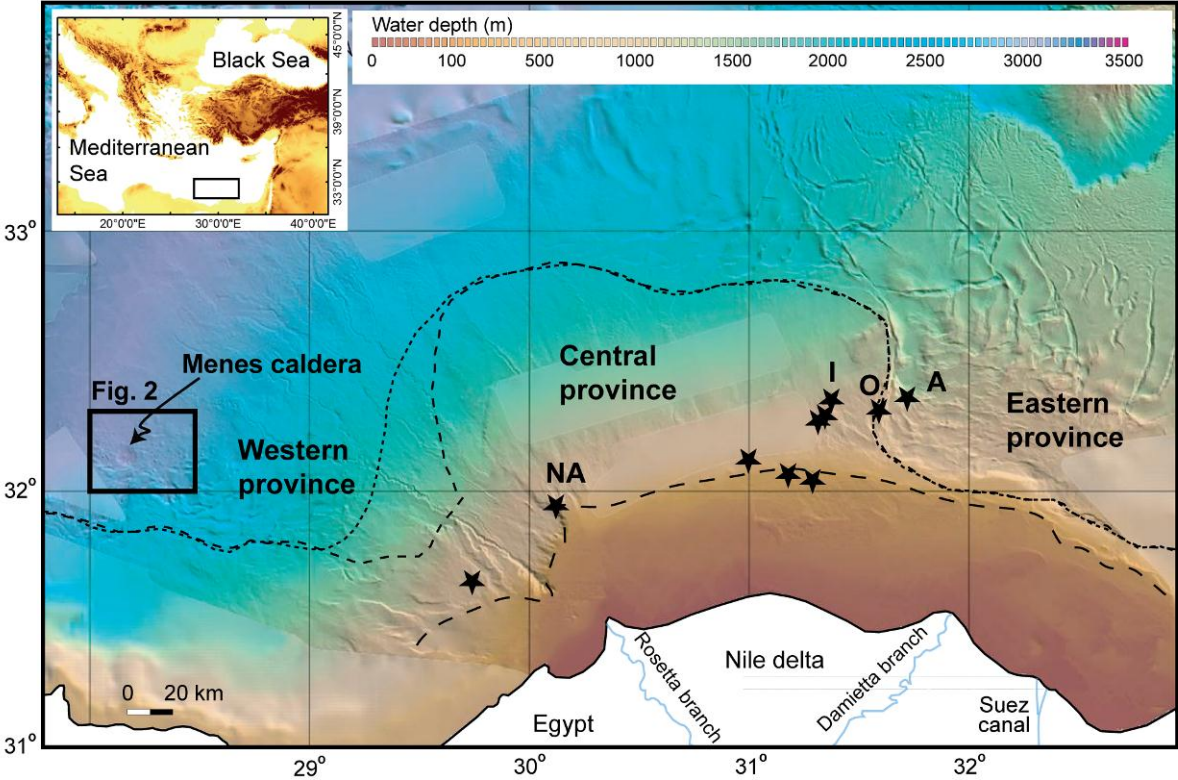


Fig. 1 Nile deep-sea fan shaded morphological map (extracted from Sardou and Mascle 2003) with locations of the Menes mud volcano caldera complex (present study) in the western Nile province at ~3,020 m water depth, and some key neighbouring MVs (stars) examined in earlier work (Loncke et al. 2004; Dupré et al. 2007, 2008b, 2010). *Coarsely hatched line* Present-day platform boundary (Loncke 2002). *Finely hatched line* Messinian eroded shelf edge and *dotted line* southward pinch-out of mobile evaporites (Loncke et al. 2006). NA, I, O and A: North Alex, Isis, Osiris and Amon mud volcanoes respectively

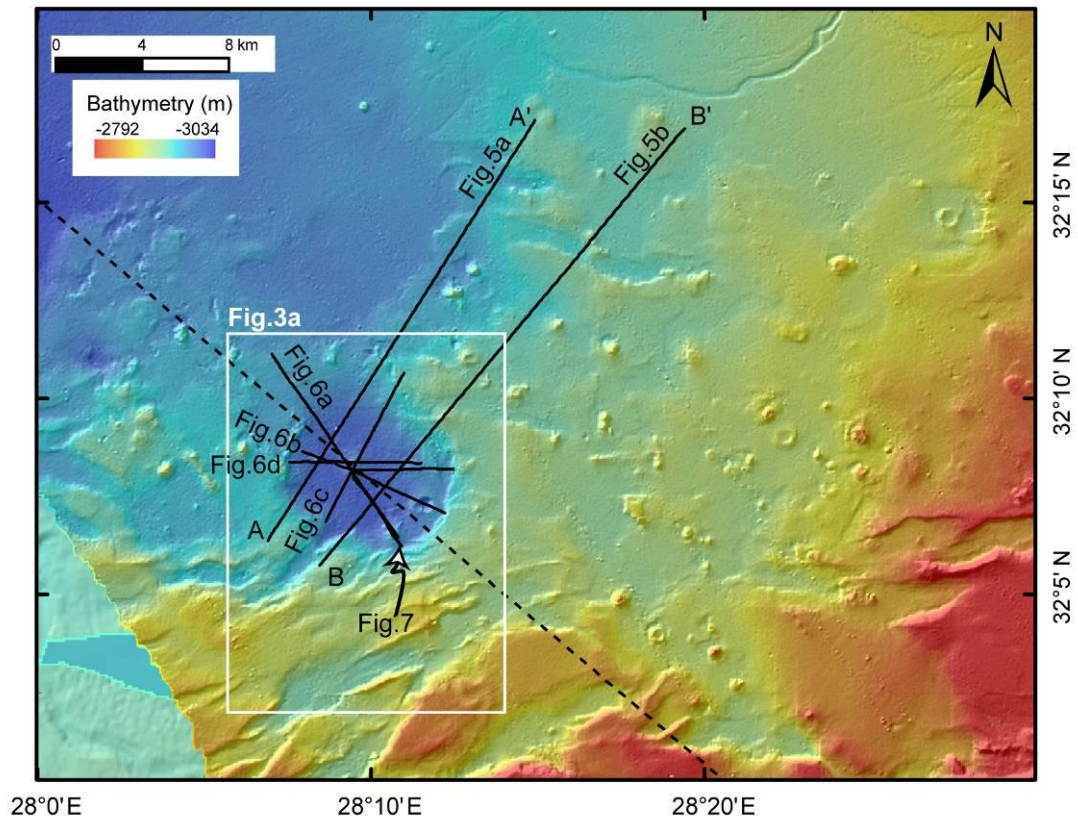


Fig. 2 Shaded bathymetry map of the Menes caldera and surroundings acquired during the FANIL expedition of 2000 (50 m grid, 30 kHz Simrad EM300 multibeam; extracted from Sardou and Mascle 2003), showing numerous morphological features of various scales (mounds, craters) related to mud volcanism. *Dashed line* Location of 2D industry seismic profile of Loncke et al. (2004), *other lines* locations of two 2D high-resolution seismic profiles (Fig. 5) and five chirp profiles (Figs. 6 and 7) of the present study

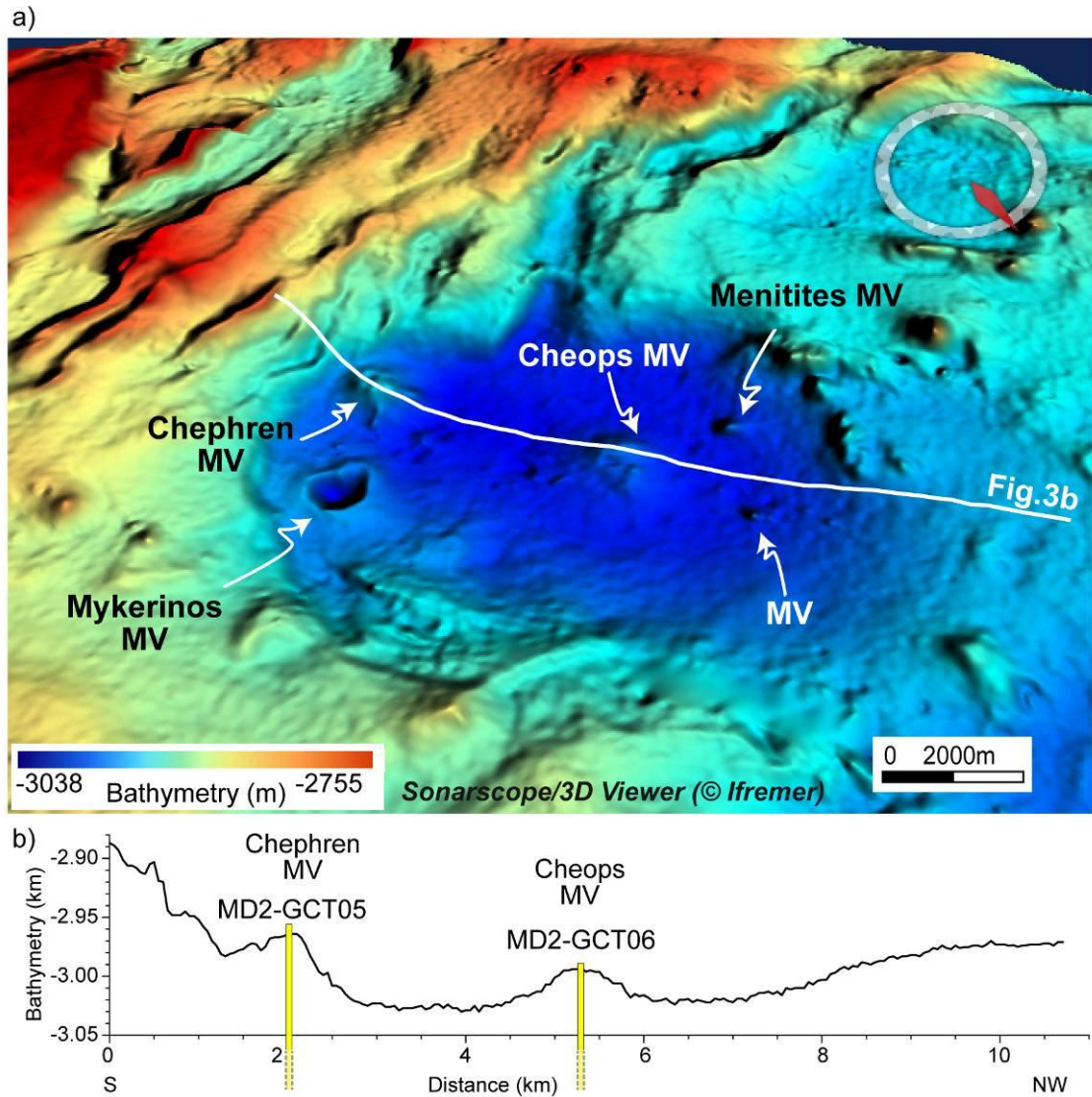


Fig. 3 a) Oblique 3D bathymetric landscape view of the Menes caldera shaded from the NE (extracted from Sardou and Mascle 2003), showing the Mykerinos, Chephren, Cheops and Menitites MVs (red arrow points to N). **b)** Bathymetric profile across the Menes caldera (cf. white line in a). *Yellow bars* Locations of temperature profiles reported in Figs. 8 and 9

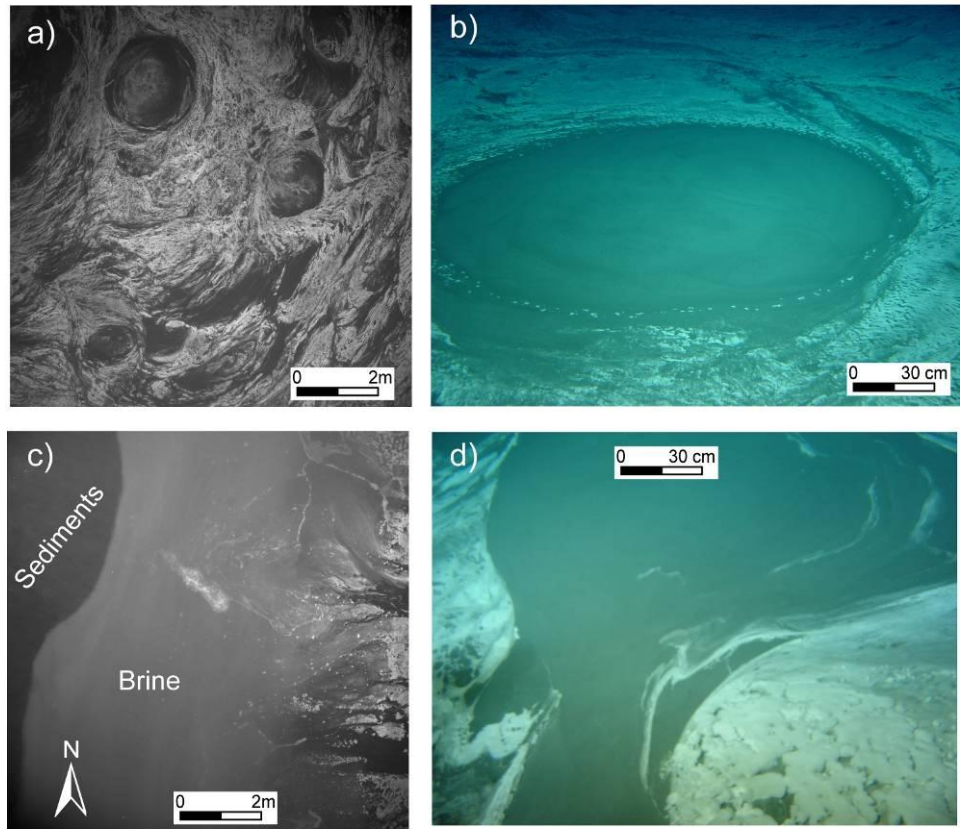


Fig. 4 Near-bottom seabed photographs (© Ifremer) at the Cheops (**a, b**) and Chephren MVs (**c, d**) taken in 2007 (**a–c**) and 2003 (**d**). **a**) Complex brine lake surface pattern resulting from upward flow of muddy brine, dense colonization by sulphide-oxidizing bacteria (*lighter shading* white filaments; cf. Omeregie et al. 2008) and ductile deformation. **b**) Recent upward flow of muddy brine, associated with a circular area not colonized by bacteria. **c**) Clear transition from fringing sediments to the brine lake at the western edge of the Chephren MV. **d**) Muddy brine outflowing at the surface of the Chephren brine lake

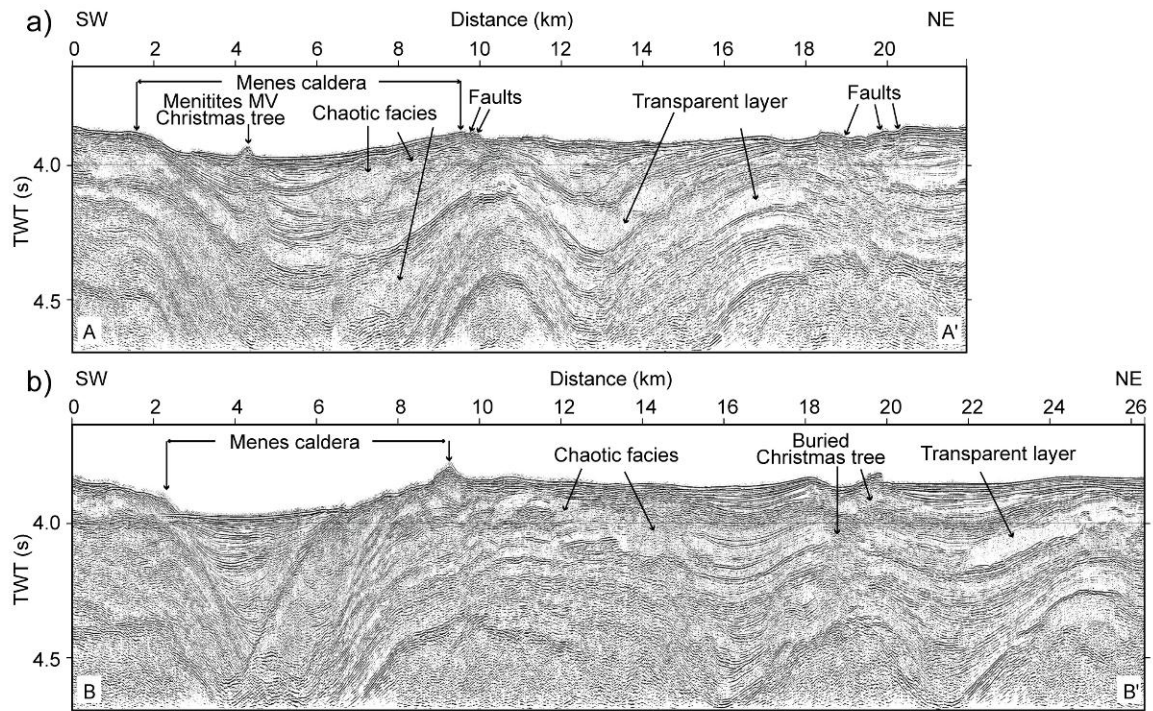


Fig. 5 High-resolution processed multichannel seismic lines (vertical exaggeration $\sim 6.5\times$) acquired across the Menes caldera and adjoining seafloor during the Fanil expedition of 2000 (see locations in Fig. 2)

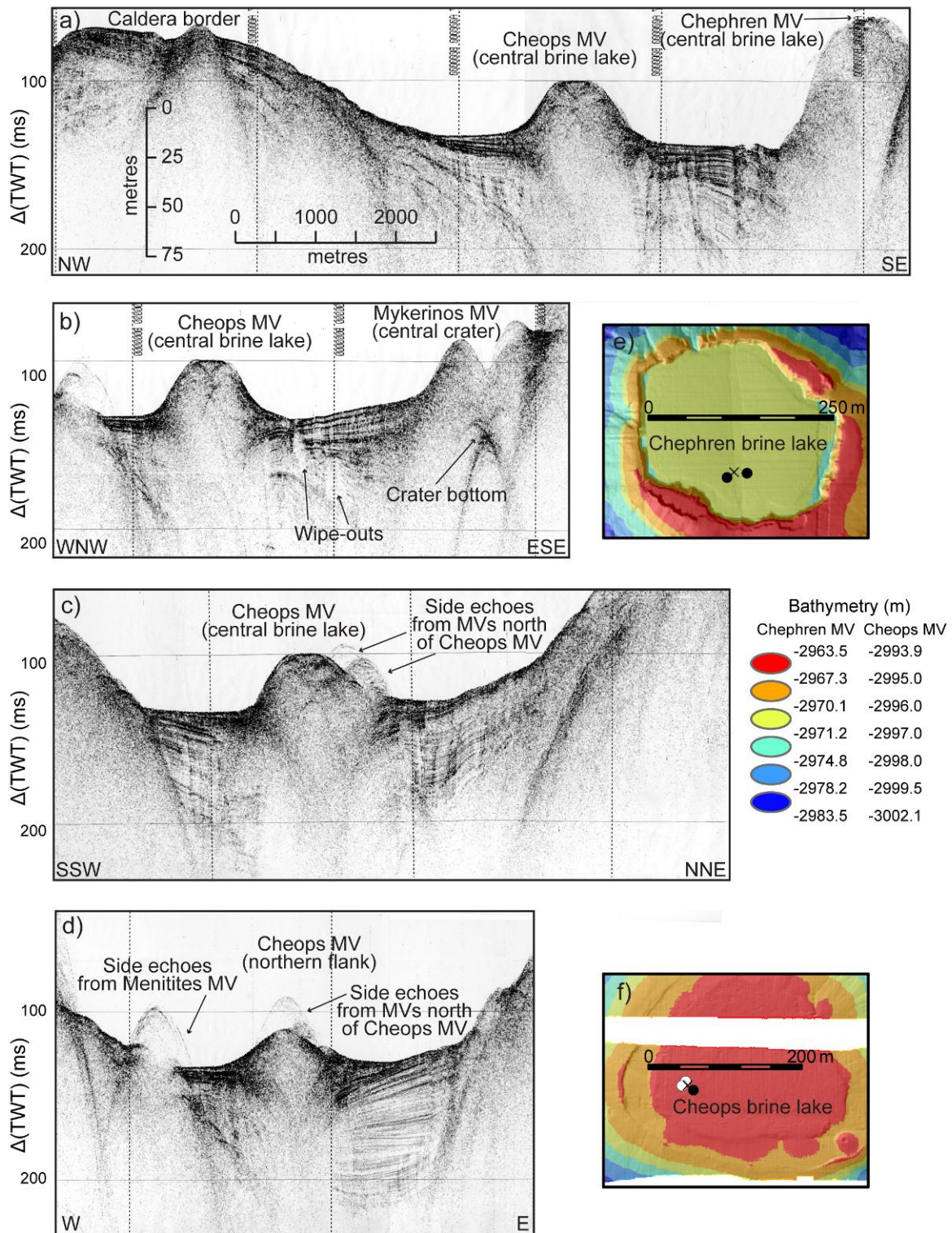


Fig. 6 a–d Four 3–5 kHz chirp profiles acquired during the 2004 Mimes expedition onboard the R/V *Pelagia* across the Cheops, Chephren, Mykerinos and Menitites MVs of the Menes caldera: **a)** MS31ES1, **b)** MS31ES2, **c)** MS42ES1 and **d)** MS54ES2 (see locations in Fig. 2; same vertical exaggeration for all profiles). **e, f)** High-resolution (1 m pixel grid) bathymetry of the summits of the **e)** Chephren and **f)** Cheops MVs, showing the flat surfaces of the brine lakes (light green and red respectively) with variations of <1 m in depth. *Black dots* Core stations of Medeco2 expedition in 2007; *white dots* core stations and *crosses* CTD stations of Mimes expedition in 2004

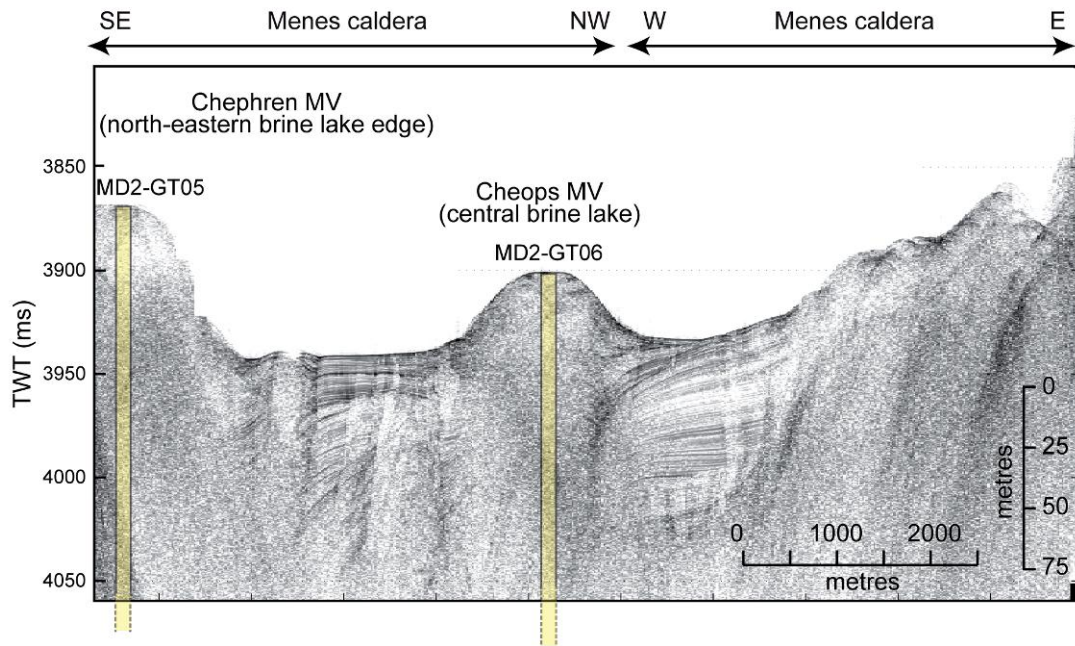


Fig. 7 Processed 1.8–5.3 kHz chirp profile (MD2CH47-48) acquired during the 2007 Medeco2 expedition onboard the R/V *Pourquoi pas?* across the southern sector of the Menes caldera (see location in Fig. 2), also showing the projected locations of cores MD2-GCT06 and MD2-GCT05 collected (respectively) 100 and 70 m from the profile

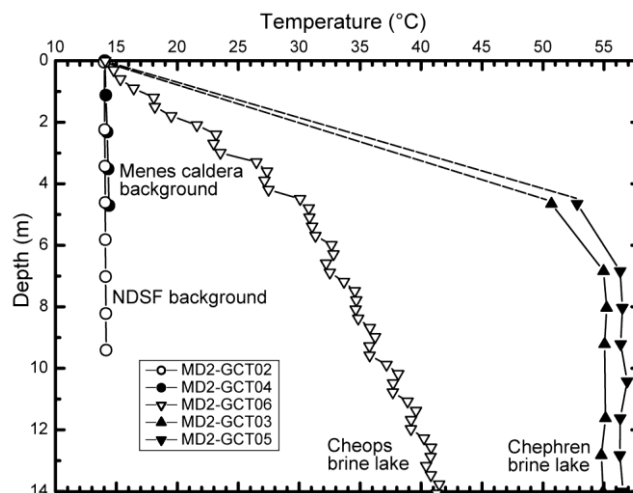


Fig. 8 Temperature profiles recorded at 0–14 m depth in bottom sediments and brine lakes during the 2007 Medeco2 expedition, comprising a background site outside of MVs in the Menes caldera, three sites in the Cheops and Chephren MV brine lakes, and a seep-free background site (*NDSF*) in the central province of the Nile deep-sea fan (see Table 2, and Figs. 1, 3 and 7 for locations)

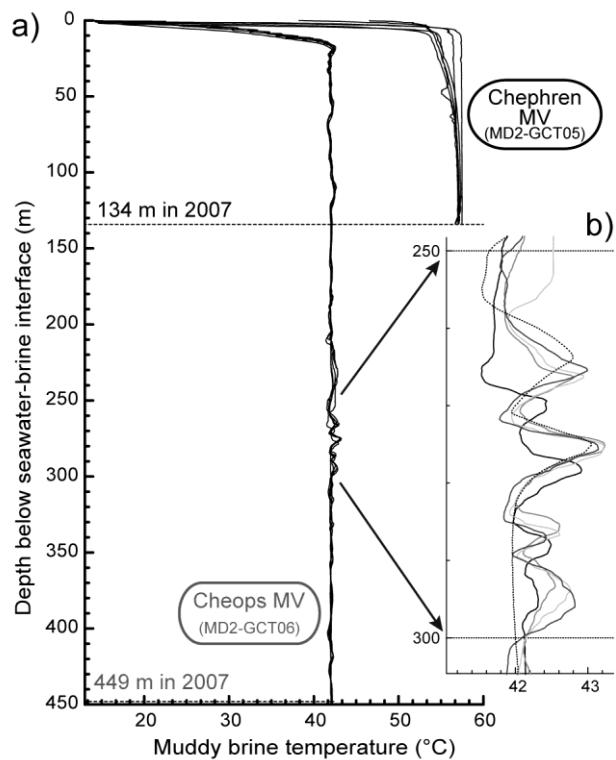
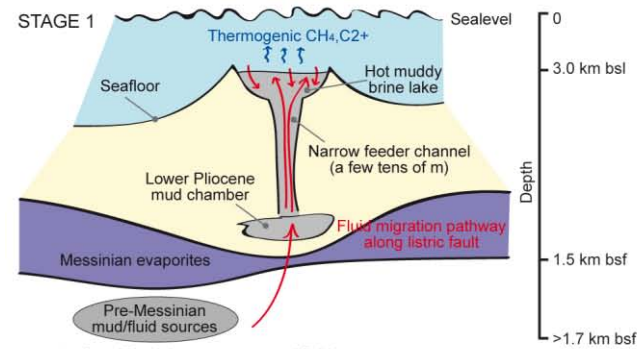
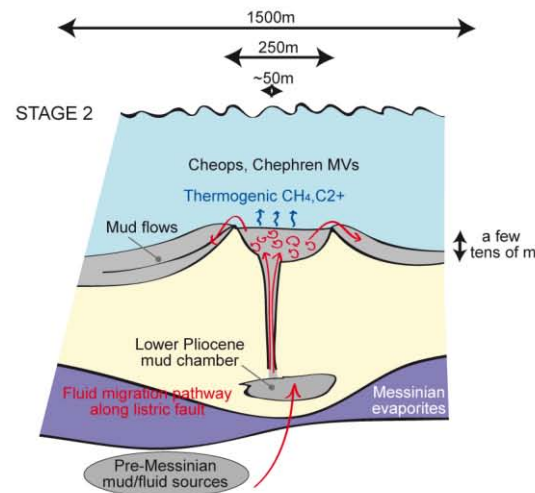


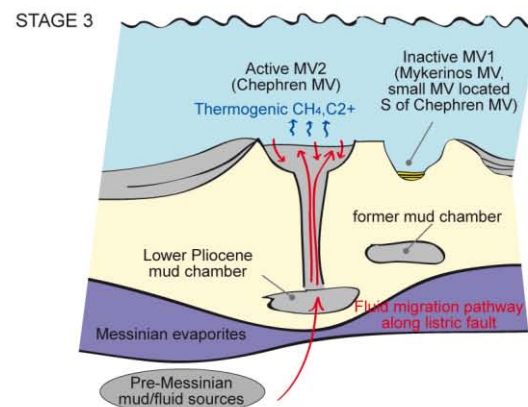
Fig. 9 a) Temperature profiles acquired in 2007 (Medeco2 expedition) within the brine lakes of Cheops MV (core MD2-GCT06, six thermometers), down to 449 m below the lake surface, and Chephren MV (core MD2-GCT05, five thermometers) down to 134 m below the lake surface (see locations in Figs. 2, 6e and f, Table 2). **b)** Zoom of the Cheops MV temperature profile at 250–300 m brine lake depths



- ascent of pre-Messinian overpressured fluids
- mud through the Messinian evaporites being enriched in brines
- mud chamber generation in the Early Pliocene sequence
- sub-vertical ascent of the warm and methane-rich muddy brines up to the seabed
- escape of thermogenic gases in the water column
- depression at the seabed created by subsidence in response to collapse of sediments
- filling with muddy brines of the newly-formed crater
- building-up of the mud volcano edifice with mud outflows at the edge of the crater



- persistence of the feeding and seepage activity
- highly-dynamic system with a very efficient mixing of the muddy brines
- growing of the mud volcano edifice
- expulsion of warm muddy brine outflows at the seabed
- possible lateral migration of the main feeder channel within the brine lake due to readjustment in the mud chamber



- possible lateral migration of the main feeder channel away from the vertical of MV1
- creation of another mud volcano MV2 with a crater at the summit filled with muddy brines
- cessation of the feeding at the vertical of MV1, emptying of the brine lake by sinking of the material, possibly enhanced by fractures within the crater, and subsequent pelagic sedimentation filling the bottom of the crater

Fig. 10 Schematic diagrams conceptualising the functioning and evolution of mud volcanoes associated with brine seepage based on the data and interpretations of the present article (*bsl* below sea level, *bsf* below seafloor, *light yellow* Plio-Quaternary deposits, *darker yellow* Recent pelagic sediments, *blue* seawater)